World Scientific
www.worldscientific.com

NEW PHYSICS AND INVISIBLE DECAY OF ORTHOPOSITRONIUM

PAOLO CRIVELLI

Institute for Particle Physics, ETH–Zürich, CH-8097 Zürich, Switzerland
paolo.crivelli@cern.ch

We propose an experiment to search for invisible decays of orthopositronium (o-Ps) with the 90% confidence sensitivity in the branching ratio as low as 10^{-8}. Evidence for this decay mode would unambiguosly signal new physics: either the existence of extra–dimensions or fractionally charged particles or new light gauge bosons. The experimental approach and the detector components of the proposed experiment are described.

Keywords: Positronium; new physics; extra–dimension; milli–charged particles.

1. Motivation

The Standard Model (SM) is very successful, but is not yet a complete theory. There are several fundamental questions, which require a physics beyond the SM for a solution. Among them are e.g. the hierarchy problem, the origin of the charge quantisation and the dark matter composition. Although the new physics is expected typically at high energies, some models predict phenomena at low energies that might be observed in rare decays of the positronium, e.g. into a photon and an axion, a new particle introduced for the solution of the strong CP problem, for a review see Refs. 1, 2.

Positronium, the positron-electron bound state, is the lightest known atom, which is bound and self-annihilates through the same, electromagnetic interaction. At the current level of experimental and theoretical precision this is the only interaction present in this system, see e.g. Refs. 1, 2. This feature has made positronium an ideal system for testing the accuracy of the QED calculations for bound states, in particular for the triplet (1^3S_1) state of Ps, orthopositronium $(o - Ps)$. Due to the odd-parity under C-transformation $o - Ps$ decays predominantly into three photons. As compared to the singlet (1^1S_0) state (parapositronium), the the long lifetime of o–Ps of $o - Ps$ decay, (due to the phase-space and additional α suppression factors) gives an enhancement factor $\simeq 10^3$, in the sensitivity to an admixture of new interactions, which are not accommodated in the SM.

This paper is focused on the search for $o - Ps \rightarrow invisible$ decay, i.e. process which is not accompanied by energy deposition in a detector. Within the SM orthopositronium can decay invisibly into a neutrino-antineutrino pair. The

$o - Ps \to \nu_e \bar{\nu}_e$ decay occurs through W exchange in the t–channel and $e^+ e^-$ anni-
hilation via Z. The decay width is[3]

$$\Gamma(o - Ps \to \nu_e \bar{\nu}_e) \approx 6.2 \cdot 10^{-18} \Gamma(o - Ps \to 3\gamma) \qquad (1)$$

For other neutrino flavours only the Z-diagram contributes. For $l \neq e$ the decay
width is[3]

$$\Gamma(o - Ps \to \nu_l \bar{\nu}_l) \approx 9.5 \cdot 10^{-21} \Gamma(o - Ps \to 3\gamma) \qquad (2)$$

Thus, in the SM the $o - Ps \to \nu \bar{\nu}$ decay rate is very small and evidence for in-
visible decays would unambiguously signal the presence of new physics. It may be
worthwhile to remember that the process with analogous experimental signature,
$Z \to invisible$ decay plays a fundamental role in the determination of the number
of lepton families.

The new models that are relevant to the $o - Ps \to invisible$ decay mode predict
the existence either of i) extra-dimensions,[2,4] or ii) fractionally charged particles,[5]
or iii) a new light vector gauge boson,[1] or iv) dark matter of the mirror matter
type.[6,7] The required sensitivity in the branching ratio $Br(o - Ps \to invisible)$ for
the possible observation of these phenomena has to be at least as low as 10^{-8}.

Note that the first experiment to search for invisible channels of o–Ps was per-
formed a long time ago.[8] The best present limit for the branching ratio, set in 1992
by Mitsui et al.[9] is

$$Br(o - Ps \to invisible) < 2.8 \times 10^{-6} \qquad (3)$$

The paper is organized as follows. In Section 1 the physics of items i)–iii) is
briefly discussed, the search for the mirror matter requires the experiment to be
performed in vacuum, for more details see Refs. 7, 10. The proposed experiment, its
setup components and the expected sensitivity are discussed in Sections 2, 3 and 4
respectively. Section 5 contains concluding remarks.

1.1. *Extra dimensions*

Models with infinite additional dimensions of Randall-Sundrum type (brane-world
models) with a big compactification radius[11−14] could provide the natural solution
to the gauge hierarchy problem.

Recently Dubovskj, Rubakov and Tinyakov[4] pointed out that in R–S brane
world models with localized bosons, massive gauge bosons localized to the Plank
brane are always unstable. The reason is that bulk modes can have arbitrarily small
masses. Any massive mode localized to the brane is then kinematically allowed to
decay into these modes.

In a recent paper Gninenko, Krasnikov and Rubbia[2] applied this mechanism to
calculate the decay of o–Ps into invisible bulk mode and obtained

$$Br(o - Ps \to \gamma^* \to additional \ dimension(s)) = \qquad (4)$$
$$\frac{9\pi}{4(\pi^2 - 9)} \cdot \frac{1}{\alpha^2} \cdot \frac{\pi}{16} \left(\frac{m_{o-Ps}}{k}\right)^2 \approx 3 \cdot 10^4 \left(\frac{m_{o-Ps}}{k}\right)^2$$

For a solution of the gauge hierarchy problem the parameter k is expected to be $k \leq O(10)\ TeV$. Indirect measurements at LEP of the $\Gamma(Z \rightarrow invisible)$ decay width constrain the parameter to $k \geq 2.7\ TeV$. Using this bound one can find

$$Br(o - Ps \rightarrow additional\ dimension(s)) \leq 0.4 \cdot 10^{-9} \qquad (5)$$

The direct LEP measurements of $\Gamma(Z \rightarrow invisible)$ results in a less stringent limit.[1,2]

$$Br(o - Ps \rightarrow additional\ dimension(s)) \leq 8 \cdot 10^{-8} \qquad (6)$$

These estimates show that the region of $\simeq 10^{-8} - 10^{-9}$ for the branching ratio is of great interest for the observation of extra–dimensions.

1.2. *Millicharged particles*

In 1986 Holdom[5] showed that grand unified models can be constructed in a natural way, adding a second, unobserved, photon to the interaction Lagrangian. In this type of model particles with an electric charge very small compared to the electron, are predicted. If such milli-charged particles exist with a small mass, the $o - Ps$ could decay apparently invisibly, since the particles would mostly penetrate any type of calorimeter without interaction. The corresponding decay width is[15]

$$\Gamma(o - Ps \rightarrow X\bar{X}) = \frac{\alpha^5 Q_X^2 m_e}{6} \cdot k \cdot F(\frac{m_X^2}{m_e^2}), \qquad (7)$$

where Q_X is the electric charge of the X-particle ($Q_e \equiv 1$), $k = 1$, $F(x) = (1 - \frac{1}{2}x)(1 - x)^{\frac{1}{2}}$ for spin $\frac{1}{2}$ and $k = \frac{1}{4}$, $F(x) = (1 - x)^{\frac{3}{2}}$ for a spin-less X-particle. For spin $\frac{1}{2}$ millicharged X-particles and $m_X \ll m_e$ one can find from experimental bound (3) that $Q_X \leq 8.6 \cdot 10^{-5}$.[9] Figure 1 shows, that a search for millicharged particles through the $o - Ps \rightarrow invisible$ decay with the sensitivity of $Br(o - Ps \rightarrow invisible) \simeq 10^{-8}$ would touch the parameter space which is not excluded by results of the recent direct experiment at SLAC.[16]

1.3. *New light X-boson*

A light vector X-boson with the interaction Lagrangian

$$L_X = g_X \bar{\psi} \gamma_\mu \psi X^\mu \qquad (8)$$

will also lead to invisible decays of $o - Ps$.[a] Supposing that the X-boson interacts with other particles (fermions) or (as a consequence of the Higgs mechanism) with itself and a scalar the contribution of the X-boson to the electron anomalous magnetic moment as given by the well known formula

$$\delta a_e = \frac{\alpha_X}{\pi} \int_0^1 \frac{x^2(1 - x)}{x^2 + (1 - x)\frac{m_X^2}{m_e^2}} \qquad (9)$$

---

[a]For the recent phenomenological bounds in models with a light vector X-boson related to the muon $(g - 2)$ and so-called NuTeV anomalies see, respectively Refs. 17, 18 and 19.
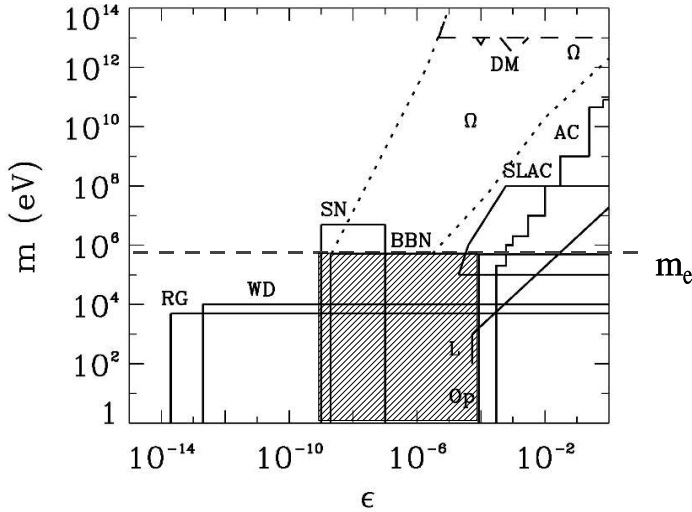
Fig. 1.   Mass–charge parameter space. The dashed region is the one which will be excluded by an experiment with a sensitivity of $\simeq 10^{-8}$.

For $m_X \ll m_e$ from the bound arising from the determination of the fine structure constant with the Quantum Hall Effect (QHE),[1] one can find that $\alpha_X < 3 \times 10^{-10}$. For the case of the heavy X-boson ($m_X \gg m_e$) the bound on the anomalous electron magnetic moment leads to the bound

$$\alpha_X \frac{m_e^2}{m_X^2} < 4.5 \cdot 10^{-10} \qquad (10)$$

For the reaction $o - Ps \rightarrow X^* \rightarrow X_1 \bar{X}_1$ (here X^* is a virtual X-boson and X_1 is a fermion (sterile neutrino) or a scalar particle) one finds that

$$Br(o - Ps \rightarrow X^* \rightarrow X_1 \bar{X}_1) = \qquad (11)$$

$$\frac{3\pi}{4(\pi^2 - 9)} \cdot k \cdot F(\frac{m_{X_1}^2}{m_e^2})(1 - \frac{m_X^2}{m_{0-Ps}^2})^{-2} \frac{\alpha_X \alpha_{XX_1}}{\alpha^3},$$

where $F(x)$ has been defined before and $\alpha_{XX_1} = g_{XX_1}^2/4\pi$. From the bound of the QHE we find for $m_X \ll m_e$ that

$$Br(o - Ps \rightarrow X^* \rightarrow X_1 \bar{X}_1) \leq k \times 2 \cdot 10^{-3} \cdot \alpha_{XX_1} \qquad (12)$$

To have an experimentally interesting branching ratio of the order $O(10^{-8})$, setting $\alpha_X = 3 \times 10^{-10}$ we must have $\alpha_{XX_1} \sim 5 \cdot 10^{-6}$.

In the opposite limit $m_X \gg m_e$ the corresponding bound reads

$$Br(o - Ps \rightarrow X^* \rightarrow X_1 \bar{X}_1) \leq k \times 3 \cdot 10^{-3} \cdot \alpha_{XX_1} \cdot \frac{m_e^2}{m_X^2} \qquad (13)$$

For an X-boson mass close to the orthopositronium mass, we have the enhancement factor $(1 - \frac{m_X^2}{m_{o-Ps}^2})^{-2}$ in formula (11) for the branching ratio, and hence, the coupling constant $\alpha_X \alpha_{XX_1}$ could be smaller.

2. Proposed Setup and Experimental Technique

In this section the design of the experiment to search for $o - Ps \rightarrow invisible$ with a sensitivity better than 10^{-8} is presented. The main components of the detector (shown in Figs. 2, 3) are: the positron source (^{22}Na), the positron tagging system, composed of a scintillating fiber viewed by two photomultipliers (PM), the positronium formation SiO_2 target and a hermetic γ–detector. The coincidence of the PM signals (see Fig. 2) from the positrons crossing the fiber, opens the gate for the data acquisition (DAQ). In the off–line analysis the 1.27 MeV photon, which is emitted from the source simultaneously with the positron, is required to be in the trigger BGO counter (shown in Fig. 3) resulting in a high confidence level of positron appearence in the positronium formation region. A positron, which enters the SiO_2 target may capture an electron creating positronium. The calorimeter detects, either the direct 2γ annihilation in flight or the 2(3) photons from the para (ortho)–positronium decays in the target.

The occurence of the $o - Ps \rightarrow invisible$ decay would appear as an excess of events with zero–energy deposition in the calorimeter above those expected from the Monte Carlo prediction (see section 4) or from the direct background measurement.

This measurement presents a new feature of this type of experiment. The idea is to obtain a pure o–Ps decay energy spectrum by comparing two different spectra from the same target filled either with N_2 (low o– Ps quenching) or with air, where the presence of paramagnetic O_2 will quench the fraction of o–Ps in the target from 10% down to 3%, due to the spin exchange mechanism:[20]

$$o - Ps + O(\uparrow\uparrow) \rightarrow p - Ps + O(\downarrow\uparrow) \tag{14}$$
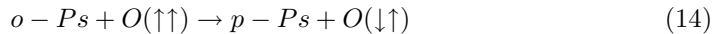
Thus the subtraction of these properly normalized spectra will result in a pure o–Ps annihilation energy spectrum in the γ–detector.

In addition, compared to the previous experiments,[8,9] the region around the target has been designed with little dead material as possible in order to reduce the photon absorbtion. The confidence level for tagging the positron appearence in the target and the efficiency of annihilation photon detection have been improved.

2.1. *Source of positrons*

The radioactive isotope ^{22}Na, which has a lifetime of 2.6 years, was chosen as a source of positrons. The positron emission from the source is accompanied by the prompt emission of a 1.27 MeV photon ($\simeq$ 3 ps delay) (see Fig. 4). This signature provides an inefficiency for positron tagging less than $\simeq 10^{-9}$. The source activity was selected based on a compromise between required trigger rate and a decrease
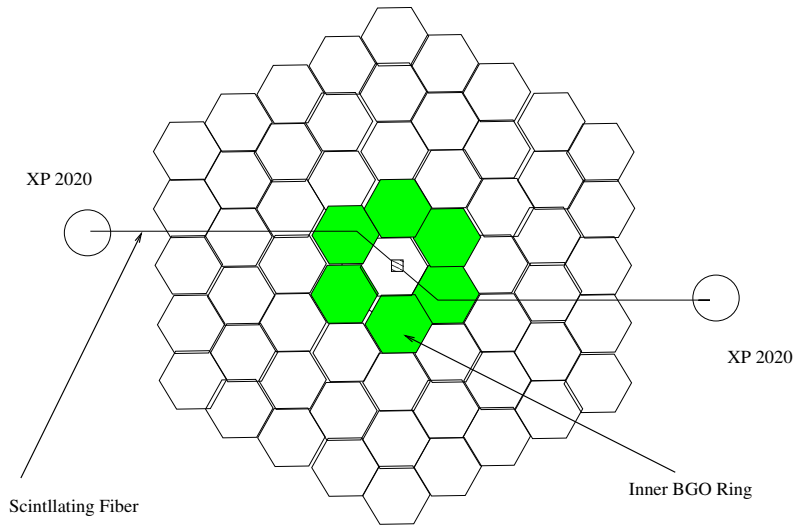
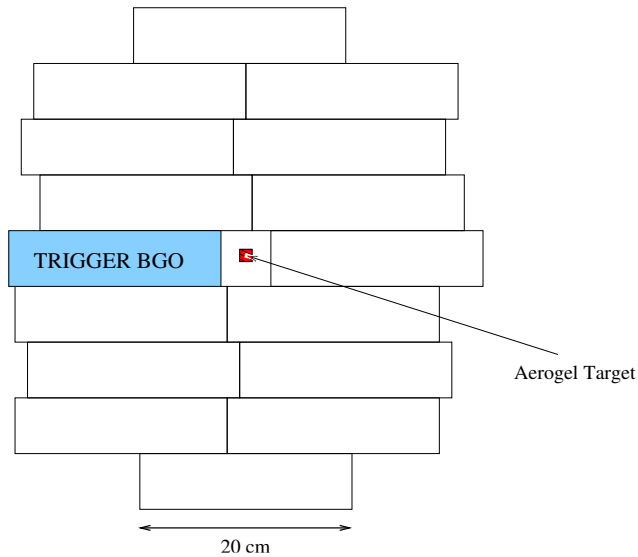Fig. 2.   Front view of the calorimeter.

Fig. 3.   Side view of the calorimeter.

in the signal efficiency due to the overlap of events close in time (pile up effect). The optimal source activity has been determinated to be about 50 kBq, for which, according to the simulation, the signal efficiency drops down to 84% (the signal of $o - Ps \rightarrow invisible$ is defined as an event depositing less than 50 keV in the γ–detector). In 10% of the cases the 1.27 MeV photon from the source is emitted due to the electron capture (EC), without positron emission. As discussed in the
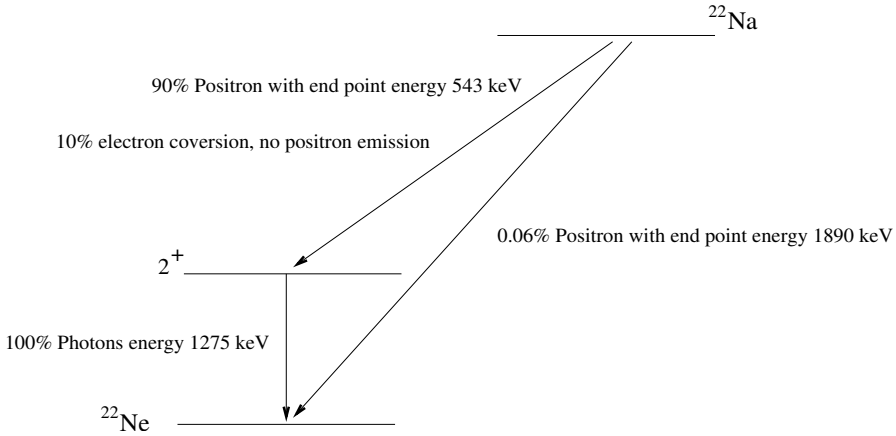
Fig. 4. Decay scheme of ^{22}Na

next section, this process introduces background related to the source container material, which was eliminated by depositing the radioactive isotope directly on the scintillating fiber. A comparison between ^{22}Na and other β^+ radioactive isotopes with a sufficient long lifetime has been made to combine the required confidence level for positron tagging with the minimal amount of dead target material and a high stopping efficiency of positrons in the target. Taking all these considerations into account, we conclude that the ^{22}Na is the best compromise for our measurements.

2.2. *The positron tagging system*

The tagging system for the experiment was designed in order to have a confidence level for the positron appeerence better than 10^{-9}. It is composed of a thin scintillating fiber viewed by two read–out PM's. It provides a relatively high efficiency and a small amount of dead material.

2.2.1. *The scintillating fiber*

For a good positron tagging efficiency, the attenuation length and the light yield of the fiber are crucial parameters. After testing the response of different scintillating fibers, the Bicron BFC 12 with a diameter of 0.5 mm has been selected. They have been prefered over the 1 mm fibers used in the experiment[21] for the less material and the possibility to have a more hermetic calorimeter, due to the smaller holes between the crystals, in which the fiber has to penetrate, since the signal has to be transported outside the calorimeter volume. Similar to experiment[21] the fiber is squeezed in the middle to get a thickness of about 100 μm. The ^{22}Na spot is deposited in the middle of the squeezed region. The measured efficiency for positron detection is slightly less than 50%.

2.2.2. *The photomultipliers*

The PM's XP 2020 have been chosen for their low noise and for their spectral sensitivity, that fits the emission spectrum of the fiber. The use of two PM signals in coincidence substantially decreases the probability of accidental coin cidences with the 1.27 MeV down to 3.2×10^{-11} (see section 3). In the future we plan to test Hamamatsu H3165-11 PM's with base R647, because of their high efficiency for single photon counting.[b]

2.3. *Positronium production target*

A SiO_2 aerogel hemisphere with a radius of 5 mm and a density of 0.1 g/cm^3, where positronium can be formed with about 7% probability, is used as a target. The aerogel is a porous material, where the o–Ps migrating in the intergranular space can decay almost freely. The dimension has been optimised to minimize the dead material, while keeping, enough material to stop positrons efficiently. The simulation shows that the probability that more than 900 keV photon energy is absorbed in it, for the given dimension, is less than 10^{-10}. Before its installation the aerogel is evacuated in a vacuum chamber (10^{-3} Torr) and backed out for 2 hours to remove the water from the pores. Then the target is filled either with high purity Nitrogen or with air.

2.4. *Calorimeter*

The optimal choice of the γ–detector (ECAL) can be made by the following considerations. The total ECAL mass W is given roughly by

$$W \simeq 4\pi/3\rho L^3 \tag{15}$$

where ρ and L are respectively mass density and the radius of the ECAL detector. We chose $L \simeq 20\lambda_{511}$, where λ_{511} is the attenuation length of 511 keV γ's. The relevant parameters for different types of materials used in ECAL's are listed below in Table 1.

Table 1.   Comparison between different types of ECAL.

ECAL type	BGO	NaI	CsI(Tl)	Sc plastic/liquid
Attenuation length, at 511 keV	$\simeq$1 cm	$\simeq$2.5 cm	$\simeq$1.9 cm	$\simeq$10 cm
density, g/cm^3	7.1	3.6	4.5	1.0
Required ECAL mass, kg	$\simeq$240	$\simeq$1890	$\simeq$1034	$\simeq$33510
Light yield, N_γ/511keV	$\simeq 4 \cdot 10^3$	$\simeq 20 \cdot 10^3$	$\simeq 10 \cdot 10^3$	$\simeq 2 \cdot 10^3$
Hygroscopic	no	yes	yes/slightly	no

The required mass is minimal for a BGO ECAL due to its high effective Z (remember, the photo-absorption cross-section $\sigma \sim Z^5$). Another important feature

[b]I would like to thank Dr. S. Asai for his advice.[9]

of BGO's is that they are not hygroscopic, thus, no additional dead material has to be introduced. For the crystal wrapped in aluminized mylar the light yield was measured to be 200 ± 14 photoelectrons/1 MeV. This results in a probability of zero energy detection due to Poisson fluctuation of the number of photoelectrons, to be less than 10^{-11} for the zero energy signal defined as events with energy deposition less than 50 keV.[21] This result justifies the selection of the BGO as the γ–detector. The crystals, which have been lent to us by the Paul Scherrer Institute (Villigen, Switzerland), have a hexagonal shape with a length of 20 cm and an outer diameter of 5.5 cm, their original wrapping is a 0.75 mm thick teflon. In order to reduce this amount of dead material, the inner ring of BGO's has been wrapped in a 2 μm thick foil, aluminized from both side with 1000Å thick layers. The required number of crystals ($\simeq 100$), determined with the simulations, provides an almost isotropically uniform thickness of 20–22 cm of BGO.

2.5. *Monitoring*

Every crystal is equipped with a LED, fired with a pulser, to monitor the crystals response. The gas and light tight box is thermally stabilised to $\pm1^oC$. The HV for every PM is measured periodically during the run.

2.6. *Data acquisition*

The data acquisition is opened by the gate generated from the coincidence between the two XP 2020 of the scintillating fiber. The gate has a lenght of 3.3 μs in order to get the probability of o–Ps decaying after this time at the level of 10^{-11}. The energy of each crystal and the signals for the two XP 2020 are recorded with four CAEN QDC's v792. The timing for the two PM's, the endcups and the internal ring is recorded by a LeCroy 1182 TDC. The VME crate is interfaced to PC with a National instruments VXI-MXI2 system and the data are acquired with LabView. The monitoring is done by another computer using ROOT, not to slow down the data acquisition.

3. Background

The main background sources, summarized in Table 2, can be subdivided in to three different types:

(i) A real trigger accompanied by annihilation energy losses.

    (a) Hermiticity: as pointed out in the previous section (Table.1), the 511 keV photons have an attenuation lenght of about 1cm in BGO. For 20 cm BGO the escape probability is about 10^{-9}.

    (b) Absorption of photons in dead material: some energy of the photons can be absorbed either in the target or/and in the wrapping of the crystals or/and in the fiber.

(c) Absorption of photons in the trigger energy window: the resolution of the endcup at 1.27 MeV is about 16% FWHM. If one (or more if e.g. one photon is backscattered in the target) of the positronium decay or direct annihilations photons overlap with the 1.27 MeV in a crystal it can be absorbed in the trigger energy window due to statistical fluctuation the energy of the photon.

(ii) A fake trigger, with no positron in the detector, can be produced by the EC 1.27 MeV photon. This gives two sources of background:

(a) the 1.27 MeV photon can scatter with an electron in the fiber and the electron can deposits some fraction of its energy in the fiber and opens the gate for the DAQ. In this case the background level is about 10^{-6}. To reduce it, a trigger requires the coincidence between the signal from the fiber and the signal from the opposite (to the direction of the positron entering the fiber and the aerogel) endcup counter. This reduces the background by one order of magnitude. The next step is to supress the background related to the 1.27 MeV photon scattering in the material, which surrounds the source, by depositing the ^{22}Na directly on the fiber. This lowers the background by another order of magnitude. The remaining background is associated with the 1.27 MeV EC photon scattering back to the trigger BGO (this photon will have between 200–300 keV energy) and a Compton electron multiple scattering in the fiber hitting the same trigger counter. This seems to be the most dangerous background for our experiment. A possible solution, which is under study, will be discussed in Section 6.

(b) The other possibility is that this photon may accidentally coincide with a fake positron trigger generated by the PM noise.

(iii) Physical backgrounds:

(a) single photon or photonless decays of o–Ps ions: $o - Ps^- \rightarrow e^- + \gamma$, $o - Ps^{--} \rightarrow e^- + e^-$

(b) photonuclear absorption of annihilation photons accompanied either by photo–neutrons or by excitation of nuclear long lived states.

The detailed evaluation of this background is in progress; some preliminary estimates show that it is less than 10^{-10}. The o–Ps produced in an excited state, immediately de–excites to the ground state[22] due to the high collisional (10^4 collision/lifetime) quenching in the SiO_2. Since the experiment is not performed in vacuum the positron wave function is assumed to overlap always with an electron wawefunction. The largest lifetime of the positrons in our experiment is assumed to be those for the three photon decay of o–Ps, namely 142 ns, thus making the probability of positron not to annihilate during the 3.3 μs gate negligible.
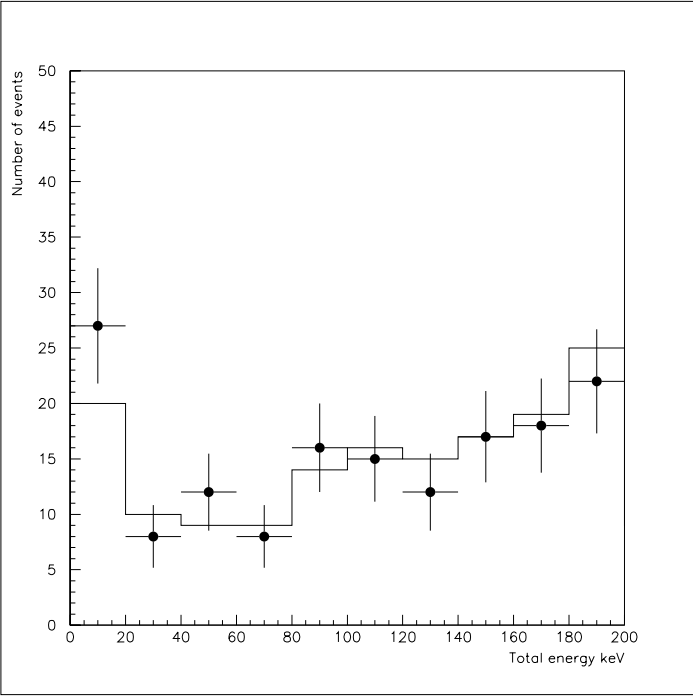
Fig. 5.   Comparison between MC simulation (points) and data of the experiment (dashed line)

4. Monte–Carlo

The feasibility of the experiment has been studied with a Monte Carlo simulation based on the code Geant 3. The simulation was cross–checked and tuned with our previous search of an exotic three–body decay of o–Ps.[21] The inefficieny for 511 keV γ detection in the measurements was predicted to be $(1.0 \pm 0.2) \times 10^{-4}$. The comparison with the data shows an agreement within 30%. The low energy part of the spectra, shown in Fig. 5, is quite well reproduced, nevertheless more work has still to be done. The losses due to light transportation, self absorption and also the non uniformity of the crystals have to be included.

Table 2.   Background table.

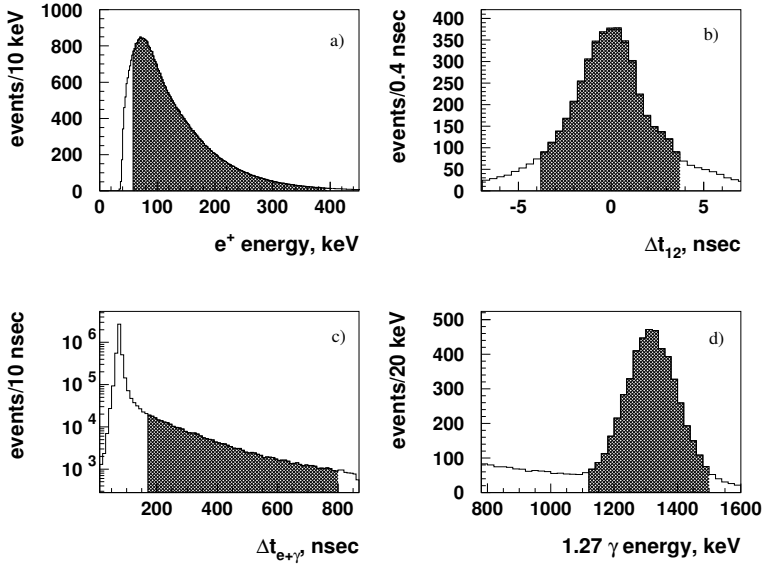| Background source	Expected level
Hermiticity	$< 10^{-10}$
Dead Material	2×10^{-10}
Absorption in trigger Energy window	10^{-10}
Compton EC photon	1.2×10^{-8}
Accidental noise and EC photon	3.2×10^{-11}
Physical backgrounds	10^{-10}

Fig. 6. Cuts for the event selection: a) Cut on the energy deposited in the scintillating fiber, b) Cut for the time difference between the two XP2020 from the fiber, c) Time spectra between start from the coincidence between the two XP and the stop from the trigger BGO, d) Energy window for 1.27 MeV photon in the trigger BGO. The shaded area corresponds to accepted events.

5. Sensitivity

As mentioned before the trigger is given by the coincidence between the signals from the two PM of the fiber. Off–line, the 1.27 MeV photon is selected in the trigger counter inside the energy window 1170–1470 keV (see Fig. 6). In order to reduce the accidental background (see previous section) the time between the coincidence and the 1.27 MeV γ is required to be inside the time window as shown in Fig. 6. A cut on the energy of the PM is applied to reduce the accidental noise. The distance between the source and the trigger BGO has been choosen to be 2 cm as a compromise between the trigger rate and the background from the Compton EC photon. The expected trigger rate for a source intensity of 50 kBq is

$$Trigger\ rate = \frac{1}{2} \cdot Positrons\ activity \cdot 5\% \cdot Fiber\ efficiency \qquad (16)$$

and knowing the fraction of o–Ps in the spectra, which is about 5%

$$Number\ of\ o-Ps/day = Trigger\ rate \cdot o-Ps\ fraction \cdot 86400s \simeq 3 \times 10^6 \quad (17)$$

Using Poisson statistics and assuming no background event observed, one can calculate the sensitivity of the experiment[23] after 60 days of running:

$$Br(o-Ps \rightarrow invisible) = 2.3/1.8 \times 10^8 \simeq 1.3 \times 10^{-8} \qquad (18)$$

6. Conclusions

With the presented type of calorimeter a background free limit for the $Br(o-Ps \rightarrow invisible)$ of $\simeq 10^{-8}$ is reacheable in about two months of data taking. Although not all the possible background sources have been identified yet, the dominant background seems to be associated with the EC photon that scatters in the fiber back to the trigger BGO counter. The accompanying Compton electron can deposit $\simeq 50$–100 keV in the fiber, which is sufficient to trigger the coincidence of the PM's signals. Since the energy deposition in the trigger counter is almost equal to the total initial energy of the 1.27 MeV photon, it is quite difficult to reject this type of events with the given resolution of the crystal. One possible way to discriminate these $e^-\gamma$ pairs is to use a thin plastic scintillator in front of the trigger BGO, with a faster timing response than the one of the BGO's. This work is in progress.

References

1. A. Rich, *Rev. Mod. Phys.* **53**, 127 (1981); S. N. Gninenko, N. V. Krasnikov and A. Rubbia, *Modern Phys. Lett.* **A17**, 1713 (2002).
2. S. N. Gninenko, N. V. Krasnikov and A. Rubbia *Phys. Rev.* **D67**, 075012 (2003).
3. A. Czarnecki and S. G. Karshenboim, hep-ph/9911410; J. Govaerts and M.Van Caillie, *Phys. Lett.* **B391**, 451 (1996).
4. S. L. Dubovsky, V. A. Rubakov and P. G. Tinyakov, *Phys. Rev.* **D62** (105011); hep-th/0006046.
5. B. Holdom, *Phys. Lett.* **B166**, 196 (1986).
6. S. L. Glashow, *Phys. Rev. Lett.* **B167**, 35 (1986).
7. R. Foot and S. N. Gninenko, *Phys. Rev. Lett.* **B480**, 171 (2000).
8. G. S. Ayotan, S. N. Gninenko, V. I. Ratzin and Yu. V. Rubakov, *Phys. Lett.* **B220**, (1989).
9. T. Mitsui, R. Fujimoto, Y. Jshisaki, Y. Ueda, Y. Yamazaki, S. Asai and S. Orito, *Phys. Rev. Lett.* **70**, 2265 (1993).

10. S. N. Gninenko, *Phys. Lett.* **B326**, 317 (1994).
11. L. Randall and R. Sundrum, *Phys. Rev. Lett.* **83**, 3370 (1990); *Phys. Rev. Lett.* **83**, 4690 (1990).
12. As a recent review, see for example: V. A. Rubakov, *Phys. Usp.* **44**, 871 (2001); *Usp. Fiz. Nauk* **171** 913 (2001); hep-ph/0104152.
13. G. F. Guidice, R. Rattazzi and J. D. Wells, *Nucl. Phys.* **B544**, 3 (1999); *Nucl. Phys.* **B595**, 250 (2001).
14. S. L. Dubovsky, V. A. Rubakov and P. G. Tinyakov, *JHEP* **0008**, 041 (2000); hep-ph/0007179.
15. M. I. Dobroliubov and A. Yu. Ignatiev, *Phys. Rev. Lett.* **65**, 679 (1990).
16. A. A. Prinz *et al.*, *Phys. Rev. Lett.* **81**, 1175 (1998).
17. S. N. Gninenko and N. V. Krasnikov, *Phys. Lett.* **B513**, 119 (2001).
18. S. Davidson *et al.*, *JHEP* **0202**, 37 (2002).
19. E. D. Carlson, *Nucl. Phys.* **B286**, 378 (1987); M. I. Dobroliubov and A. Yu. Ignatiev, *Nucl. Phys.* **B309**, 655 (1988); M. I. Dobroliubov, *Yad. Phys.* **52**, 551 (1990); *Sov. J. Nucl. Phys.* **52**, 352 (1990); S. N. Gninenko and N. V. Krasnikov, *Phys. Lett.* **B427**, 307 (1998); S. N. Gninenko and N. V. Krasnikov, *Phys. Lett.* **B434**, 163 (1998).
20. M. Kalimoto, T. Hyodo and T. B. Change, *J. Phys.* **B23**, 589 (1990).
21. A. Badertscher *et al.*, *Phys. Lett.* **B542**, 29 (2002); hep-ex/0206054.
22. J. C. Nico, D. W. Gidley, A. Rich and P. W. Zitewitz, *Phys. Rev. Lett.* **65**, 1344 (1990).
23. Review of Particle Physics, *Phys. Rev.* **D66**, 236 (2002).